Available online at www.sciencedirect.com
SCIENCE DIRECT®
Journal of Solid State Chemistry 179 (2006) 117–121
JOURNAL OF SOLID STATE CHEMISTRY
www.elsevier.com/locate/jssc

Dynamics of superionic $Rb_3H(SeO_4)_2$ single crystals studied by ^1H and ^{87}Rb spin–lattice relaxation

Ae Ran Lim[a,*], M. Ichikawa[b,1]

[a]Department of Science Education, Jeonju University, Jeonju 560-759, Chonbuk, Republic of Korea
[b]Division of Physics, Graduate School of Science, Hokkaido University, Sapporo 060-0810, Japan

Received 12 August 2005; received in revised form 5 October 2005; accepted 8 October 2005
Available online 15 November 2005

Abstract

The ^1H and ^{87}Rb spin–lattice relaxation and spin–spin relaxation times in superionic $Rb_3H(SeO_4)_2$ single crystals grown by the slow evaporation method were measured over the temperature range 160–450 K. The temperature dependencies of the ^1H T_1, $T_{1\rho}$, and T_2 are measured. In the ferroelastic phase, T_1 differs from $T_{1\rho}$, which is in turn different from T_2, although these three relaxation times converge to similar values near 410 K. This transition seems to occur at temperature which is about 40 K lower than the superionic transition temperature. The observation of liquid-like values of the ^1H T_1, $T_{1\rho}$, and T_2 in the high temperature is compatible with the phase being superionic, indicating that the destruction and reconstruction of hydrogen bonds does indeed occur at high temperature. In addition, the ^{87}Rb T_1 and T_2 values at high temperature were similar (on the order of milliseconds), a trend that was also observed for ^1H T_1 and T_2. This behavior is expected for most hopping-type ionic conductors, and could be attributed to interactions between the mobile ions and the neighboring group ions within the crystal. The motion giving rise to this liquid-like behavior is related to the superionic motion.
© 2005 Elsevier Inc. All rights reserved.

PACS: B: 81.10.−h; D: 77.80 Bh; E: 76.60 k

Keywords: Physics of crystal growth; Phase transition; Nuclear magnetic resonance and relaxation

1. Introduction

Proton-conducting solids are of interest due to their potential applications in fuel cells, steam electrolysis, and sensors [1]. Proton conduction occurs in several types of materials, including many hydrogen-bonded systems [2–8]. Hydrogen-bonded superionic crystals are well known for their proton orderings at low temperatures as well as for high protonic conductivity, which increases significantly in the high-temperature superionic phases. The increased conductivity in the high-temperature phases arises from dynamical disordering of the hydrogen-bond network, which results in an increase in the number of possible positions for protons [9]. In some ferroelectric and ferroelastic hydrogen-bonded crystals, superionic conductivity has been discovered; for example, crystals of composition $M_3H(XO_4)_2$ ($M = K$, Rb, Cs, and NH_4; $X = S$, Se) exhibit high proton conductivity in their high temperature phases [10,11]. Compounds with the general formula $M_3H(XO_4)_2$ contain very strong hydrogen bonds linking the XO_4^{2-} ions into "zero-dimensional" hydrogen bond networks consisting of isolated XO_4^{2-}–H–XO_4^{2-} dimers [12,13]. $Rb_3H(SeO_4)_2$ belongs to a family of hydrogen-bonded crystals with general formula $M_3H(XO_4)_2$. At room temperature, all such crystals are ferroelastic and isomorphous with space group $A2/a$, except for $Cs_3H(SeO_4)_2$, which has space group $C2/m$ [14]. Above room temperature, these crystals undergo a ferroelastic transition at 339–456 K to the same trigonal ($R3m$) paraelastic and superionic phase [15,16]. $Rb_3H(SeO_4)_2$ undergoes a structural phase transition at 446 K [17,18].

An NMR study of $Rb_3H(SeO_4)_2$ revealed drastic changes near $T_c = 446\,K$ in the angular dependence of

*Corresponding author. Fax: +82 63 220 2054.
E-mail addresses: aeranlim@hanmail.net, arlim@jj.ac.kr (A.R. Lim).
[1]Present address: Kitanosawa 7-1-30, Minami-ku, Sapporo 005-0832, Japan.

0022-4596/$ - see front matter © 2005 Elsevier Inc. All rights reserved.
doi:10.1016/j.jssc.2005.10.009

the ^{87}Rb quadrupole-perturbed central line of the ^{87}Rb NMR spectrum, as well as in the ^{1}H NMR spectrum [19]. These observations indicate that the structural phase transition involves the breaking of the SeO_4–H–SeO_4 hydrogen-bonded dimers and the formation of a dynamic two-dimensional H-bonded network formed by reorienting the $HSeO_4$ groups in the ab-plane. Matsuo et al. [20,21] studied the variation in proton motion at the ferroelastic–paraelastic phase transition temperatures by examining changes in the NMR line shape. Although the ^{87}Rb spin–lattice relaxation times for $Rb_3H(SeO_4)_2$ have been reported, the ^{1}H relaxation times have not yet been determined.

The spin–lattice relaxation time of a nucleus provides a measure of its dynamic properties such as the nucleus–phonon interaction, and indicates how easily the excited state energy of the nuclear system is transferred to the lattice. To obtain information about the structural phase transition and the relaxation processes that occur in $Rb_3H(SeO_4)_2$ single crystals, it is useful to measure the spin–lattice relaxation time and the spin–spin relaxation time of ^{1}H and ^{87}Rb nuclei. In the present study, we investigated the temperature dependencies of the spin–lattice relaxation time in the laboratory frame, T_1, the spin–lattice relaxation time in the rotating frame, $T_{1\rho}$, and the spin–spin relaxation time, T_2, for the ^{1}H and ^{87}Rb nuclei in $Rb_3H(SeO_4)_2$ single crystals using pulse NMR spectrometer. The correlation between the superionic motion and the relaxation time is discussed here, is a new result.

2. Crystal structure

For $Rb_3H(SeO_4)_2$, the monoclinic unit cell of the crystal belongs to the space group $A2/a$ at room temperature and is characterized by lattice parameters $a = 10.475$ (1) Å, $b = 6.090$ (1) Å, $c = 15.418$ (3) Å, and $\beta = 102.91$ (1)° [22]. The crystal structure of the ferroelastic phase of $Rb_3H(SeO_4)_2$ is shown in Fig. 1. The structure of

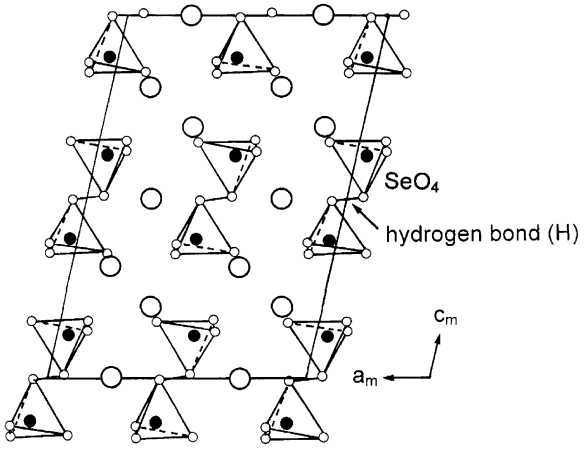

Fig. 1. Crystal structure of the $Rb_3H(SeO_4)_2$ at room temperature onto the ac-plane.

Table 1
Se–O bond lengths and O–Se–O bond angles in $Rb_3H(SeO_4)_2$

Bond type	Bond length (Å)	Bond type	Bond angle (°)
Se–O	1.632 (1)	O–Se–O	105.7 (2)
	1.701 (1)		111.9 (2)
	1.633 (1)		112.9 (2)
	1.627 (1)		105.0 (2)
			108.0 (2)
			112.7 (2)
Average Se–O length 1.648		Average O–Se–O angle 109.4	

$Rb_3H(SeO_4)_2$ is made up of hydrogen-bonded SeO_4 dimers and Rb cations. Each SeO_4–H–SeO_4 dimer consists of two slightly deformed SeO_4 tetrahedra connected by a hydrogen bond. The Se–O distances and O–Se–O bond angles of slightly deformed SeO_4 tetrahedra are given in Table 1 [23,24]. The crystal structure of the paraelastic phase belongs to the space group $R3m$, and is characterized by lattice parameters $a = 6.118$ (1) Å and $c = 22.629$ (7) Å [22,25]. In this phase, the crystal is characterized by rhombohedral symmetry and has a unit cell with hexagonal structure.

3. Experimental method

$Rb_3H(SeO_4)_2$ crystals were grown with a pseudo-hexagonal plate shape by slow evaporation of an aqueous solution containing Rb_2SO_4 and H_2SeO_4 in a molar ratio of Rb_2SO_4:H_2SeO_4 = 3:1.54. The resulting crystals were thin hexagonal plates, similar to the pseudo-hexagonal c-plates of $K_3H(SeO_4)_2$.

The nuclear magnetic resonance signals of the ^{1}H and ^{87}Rb nuclei in the $Rb_3H(SeO_4)_2$ single crystals were measured using Varian 200 and Bruker DSX 400 FT NMR spectrometers, respectively, at the Korea Basic Science Institute. The static magnetic fields were 4.7 and 9.4 T, respectively, and the central radio frequency was set at $\omega_o/2\pi = 200$ MHz for the ^{1}H nucleus and at $\omega_o/2\pi = 130.93$ MHz for the ^{87}Rb nucleus. The ^{1}H and ^{87}Rb experiments were performed using a $\pi - t - \pi/2$ pulse sequence for the T_1 measurements, a spin-locking sequence $\pi - B_1(t)$ with $B_1 = 5$ kHz for the $T_{1\rho}$ measurements, and the T_2 were measured using the Hahn spin-echo sequence. The temperature-dependent NMR measurements were obtained over the temperature range 160–450 K. The samples were maintained at a constant temperature (accuracy, ±0.5 K) by controlling the helium gas flow and the heater current.

4. Experimental results and analysis

4.1. ^{1}H spin–lattice relaxation and spin–spin relaxation times

The NMR signal for the ^{1}H nucleus ($I = 1/2$, natural abundance 100%) in a $Rb_3H(SeO_4)_2$ crystal consisted of

two resonance lines. The recovery trace of the magnetization for this crystal was measured at several different temperatures. The saturation recovery trace for the ^{1}H resonance line can be represented by the following equation [26]:

$$S(\infty) - S(t) = S(\infty)\exp(-Wt), \quad (1)$$

where W is the transition probability for $\Delta m = \pm 1$. Thus, the relaxation time, $T_1 = 1/W$, can be determined directly from the slope of the plot of $\log\{[S(\infty) - S(t)]/S(\infty)\}$ versus time (t). The saturation recovery traces could be represented by a single exponential form at all temperatures investigated. In addition, the spin–spin relaxation time, T_2, was determined, and the recovery trace of the ^{1}H resonance line can be represented as [26]

$$S(t) = \exp(-Wt), \quad (2)$$

where $T_2 = 1/W$.

The temperature dependencies of the ^{1}H T_1, $T_{1\rho}$, and T_2 are shown in Fig. 2, where magnetic field was applied along the c-axis. The spin–spin relaxation time, T_2, shows a strong temperature dependence. In the ferroelastic phase, T_1 differs from $T_{1\rho}$, which is in turn different from T_2, although these three relaxation times converge to similar values above 400 K. The decrease in $T_{1\rho}$ can be ascribed to the onset of slow translational motion of protons. As the temperature increases, ω_c (reorientation) increases, causing a narrowing of the proton NMR line-width and, as a result, T_2 increases. This increase in T_2 is due to protons rapidly moving between the oxygens of one SeO_4 group, giving rise to different, well-defined "orientations" of the $H(SeO_4)_2^{3-}$ ion. In the ferroelastic phase, ^{1}H NMR measurements of superionic compounds show $T_2 << T_{1\rho} << T_1$, with the difference of more than order of magnitude. From the temperature dependences of T_1 and T_2, we conclude that, in the ferroelastic phase, $\omega_{dip} << \omega_c$ (reorientation) $< \omega_o$. Here ω_{dip} is the proton Larmor frequency in the local dipolar field (i.e., the dipolar width of the proton line expressed in frequency units), ω_c (reorientation) is the frequency of the rotational motions of the $H(SeO_4)_2^{3-}$ group between different equilibrium orientations, ω_c (translation) is the frequency of the motions of the protons between different sites due to the translational motion, and ω_o is the Larmor frequency in an external magnetic field. At a temperature which is about 40 K lower than the superionic transition temperature, T_1 is approximately same the T_2 and $T_{1\rho}$. Therefore, this transition seems to occur at temperature near 410 K. At high temperature, there is almost no distinction between the two types of motions; the results show that T_1, $T_{1\rho}$, and T_2 becomes liquid-like near 400 K, indicating the presence of translational motion in addition to molecular reorientation. The liquid-like values of the ^{1}H T_1, $T_{1\rho}$, and T_2 are compatible with the phase above T_c being superionic.

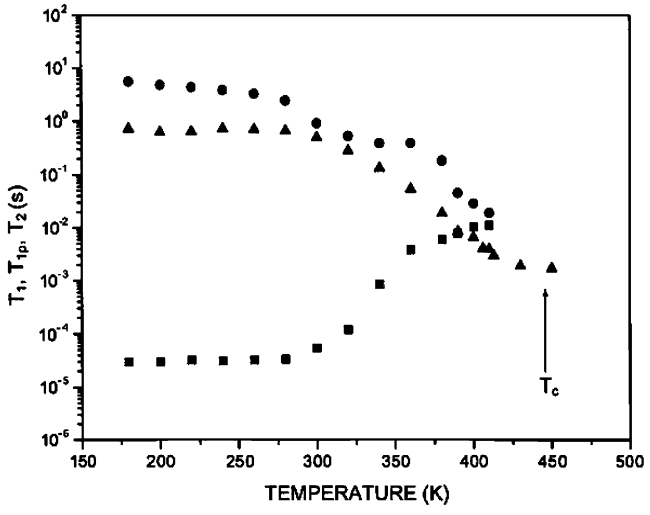

Fig. 2. Temperature dependencies of the spin–lattice relaxation time in the laboratory frame, T_1, spin–lattice relaxation time in the rotating frame, $T_{1\rho}$, and spin–spin relaxation time, T_2, for ^{1}H in a $Rb_3H(SeO_4)_2$ single crystal ((●) T_1, (▲) $T_{1\rho}$, and (■) T_2).

4.2. ^{87}Rb spin–lattice relaxation and spin–spin relaxation times

Fig. 3 shows the ^{87}Rb NMR spectrum of crystalline $Rb_3H(SeO_4)_2$ at room temperature, where the magnetic field was applied along the c-axis. When a crystal with crystallographically equivalent nuclei is rotated about the crystallographic axis, the nuclei give rise to three lines: one central line and two satellite lines. Usually, the quadrupole parameters of ^{87}Rb nuclei are large enough to be measured in MHz. Two satellite lines for the ^{87}Rb nucleus are far away from the central line. Therefore, the satellite lines are not easy to obtain. Given that $Rb_3H(SeO_4)_2$ contains three types of crystallographically inequivalent ^{87}Rb nuclei, Rb(1), Rb(2), and Rb(2′) [27], the spectrum arising from three types of rubidium nuclei would be expected to contain nine resonance lines. However, only three resonance lines are observed in the temperature range 180–410 K; these resonance lines correspond to the central transition ($+1/2 \leftrightarrow -1/2$) of the ^{87}Rb NMR spectrum for Rb(1), Rb(2), and Rb(2′). This is consistent with three nonequivalent quadrupole parameters, as found by Takeda

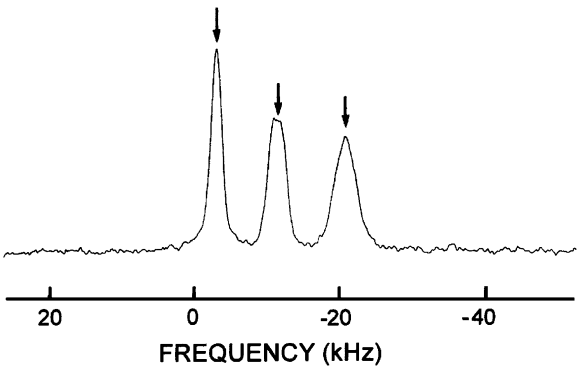

Fig. 3. ^{87}Rb NMR spectrum of a $Rb_3H(SeO_4)_2$ single crystal.

et al. [28], in the ^{87}Rb NMR spectrum of crystalline $Rb_3H(SO_4)_2$.

The spin–lattice relaxation times of ^{87}Rb in $Rb_3H(SeO_4)_2$ were measured using an inversion recovery sequence; these measurements were conducted only for the central line. The recovery trace for the central line of Rb with dominant quadrupole relaxation is not a single exponential, but can be represented by a combination of two exponential functions [29,30]:

$$S(\infty) - S(t) = 2S(\infty)[0.5\exp(-2W_1t) + 0.5\exp(-2W_2t)], \quad (3)$$

where W_1 and W_2 are the transition probabilities for $\Delta m = \pm 1$ and $\Delta m = \pm 2$. The recovery data for the temperature investigated here fits well with Eq. (3). The relaxation rates are given by

$$1/T_1 = [2(W_1 + 4W_2)]/5. \quad (4)$$

The temperature dependencies of the spin–lattice relaxation times for the three central lines of ^{87}Rb in $Rb_3H(SeO_4)_2$ were measured. The recovery traces for the three resonance lines of ^{87}Rb with dominant quadrupole relaxation can be represented by a combination of two exponential functions (Eq. (3)). The temperature dependencies of the ^{87}Rb relaxation rates W_1 and W_2 of $Rb_3H(SeO_4)_2$, displayed in Fig. 4, show that W_1 is smaller than W_2 at all temperatures, and W_1 and W_2 exhibit a similar trend with increasing temperature. Specifically, W_1 and W_2 increase slowly up to 350 K, and then rapidly increase at higher temperatures. The temperature dependence of the nuclear spin–lattice relaxation time, T_1, for ^{87}Rb is obtained using Eq. (4), and the results are shown in Fig. 5. The T_1 values for the three resonance lines are the same within the experimental error. In addition, the spin–spin relaxation time, T_2, was found to depend on temperature. As shown in Fig. 5, T_2 decreases with increasing temperature, with T_1 and T_2 taking on similar values (i.e., on the order of milliseconds) near 400 K.

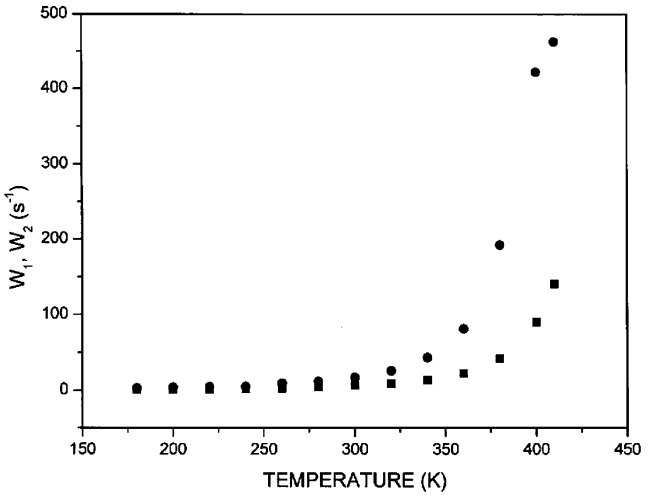

Fig. 4. Temperature dependences of the ^{87}Rb spin–lattice transition rates W_1 and W_2 of a $Rb_3H(SeO_4)_2$ single crystal ((■) W_1 and (●) W_2).

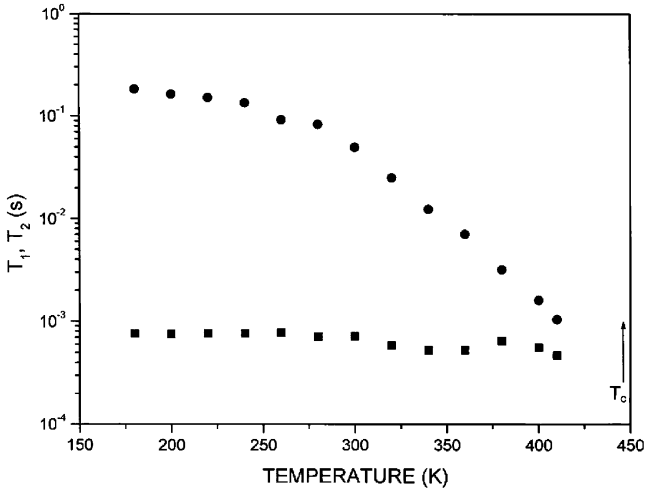

Fig. 5. Temperature dependences of the spin–lattice relaxation time, T_1, and spin–spin relaxation time, T_2, of ^{87}Rb in a $Rb_3H(SeO_4)_2$ single crystal ((●) T_1 and (■) T_2).

Unfortunately, in the present work the relaxation time in the laboratory frame could not be determined above 410 K because the NMR spectrometer did not have adequate temperature control at higher temperatures; hence, the phase transition at 446 K could not be detected in the ^{87}Rb T_1 and T_2 NMR results.

5. Discussion and conclusion

The spin–lattice relaxation time, T_1, and the spin–spin relaxation time, T_2, in the laboratory frame, and the spin–lattice relaxation time in the rotating frame, $T_{1\rho}$, for the ^{1}H and ^{87}Rb nuclei in $Rb_3H(SeO_4)_2$ single crystals were investigated with NMR spectrometer. These NMR observations provide a consistent description of the dynamics of the ^{1}H and ^{87}Rb nuclei in this material. In the low temperature, T_1 differs from $T_{1\rho}$, which is in turn different from T_2, although they converge to similar values near 410 K. At a temperature which is about 40 K lower than the superionic transition temperature, T_1, $T_{1\rho}$, and T_2 for ^{1}H were similar, and are indicative of a liquid-like system, with both translational motion and molecular reorientation. The liquid-like values of T_1, $T_{1\rho}$, and T_2 indicate that the phase near 410 K was superionic. The structural phase transition at high temperatures may involve the breaking of hydrogen bonds between the nearest SeO_4 and forming new weaker disordered hydrogen bonds between neighboring SeO_4 tetrahedra. This structural phase transition may involve significant reorientation of SeO_4 tetrahedra and dynamical disorder of the hydrogen bonds between them. In previous reports [31], the high electrical conductivity in the superionic phase of $M_3H(XO_4)_2$ (M = K, Rb, Cs, and NH_4; X = S, Se) crystals has been attributed to the hopping of protons, which is accompanied by the destruction and reconstruction of hydrogen bonds. In the case of $Rb_3H(SeO_4)_2$ crystals, the ^{1}H spin–lattice relaxation time decreases with increasing temperature, indicating that the

destruction and reconstruction of hydrogen bonds does occur at high temperatures. The variations of the ^{87}Rb T_1 and T_2 with temperature were similar to those observed for the ^{1}H T_1, $T_{1\rho}$, and T_2. This behavior was expected for most hopping-type ionic conductors, and could be attributed to interactions between the mobile ions and the neighboring group ions within the crystal. The rubidium atoms were not involved in this type of dynamics. However, the spin-interactions determining the relaxation times for both ^{1}H and ^{87}Rb nuclei were probably coupled, which means that the dynamics of the protons influence the dipolar and quadrupolar interactions controlling the relaxation time of the ^{87}Rb nuclei. This explains the similar trend in the relaxation times determined from NMR data in the ^{1}H and ^{87}Rb NMR experiments. As the temperature was increased, T_1 becomes very short and liquid-like. The motion giving rise to this liquid-like behavior may be related to the superionic motion.

Acknowledgment

This work was supported by a Korea Research Foundation Grant (KRF-2004-015-C00148).

References

[1] M. Haile, D.A. Boysen, C.R. Chisholm, R.B. Merle, Nature 410 (2001) 910.
[2] A. Kawada, A.R. McGhie, M.M. Labes, J. Chem. Phys. 52 (1970) 3121.
[3] V.H. Schmidt, J.E. Drumeheller, F.L. Howell, Phys. Rev. B 4 (1971) 4582.
[4] A.I. Baranov, L.A. Shuvalov, N.M. Schagina, JEPT Lett. 36 (1982) 459.
[5] A.I. Baranov, R.M. Fedosyuk, N.M. Schagina, L.A. Shuvalov, Ferroelectric. Lett. 2 (1984) 25.
[6] R. Blinc, J. Dolinsek, G. Lahajnar, I. Zupancic, L.A. Shuvalov, A.I. Baranov, Phys. Status Solidi b 123 (1984) k83.
[7] M. Friesel, B. Baranowski, A. Lunden, Solid State Ion. 35 (1989) 85.
[8] A.I. Baranov, B.V. Merinov, A.V. Tregubchenko, V.P. Khiznichenko, L.A. Shuvalov, N.M. Schagina, Solid State Ion. 36 (1989) 279.
[9] N.I. Pavlenko, J. Phys.: Condens. Matter 11 (1999) 5099.
[10] K. Gesi, J. Phys. Soc. Jpn. 48 (1980) 886.
[11] A.I. Baranov, A.V. Tregubchenko, L.A. Shuvalov, N.M. Schagina, Fiz. Tverd. Tela. 29 (1987) 2513.
[12] M. Ichikawa, T. Gustafsson, K. Motida, I. Olovsson, K. Gesi, Ferroelectrics 108 (1990) 307.
[13] M. Ichikawa, T. Gustafsson, I. Olovsson, J. Mol. Struct. 321 (1994) 21.
[14] M. Ichikawa, T. Gustafsson, I. Olovsson, Solid Sate Commun. 78 (1991) 547.
[15] A.I. Baranov, A.V. Tregubcenko, L.A. Shuvalor, N.M. Shchagina, Sov. Phys. Solid State 29 (1987) 1448.
[16] B.V. Merinov, A.I. Baranov, L.A. Shuvalov, Sov. Phys. Crystallogr. 35 (1990) 200.
[17] A.I. Baranov, I.I. Makarova, L.A. Tregubcenko, L.A. Shuvalor, V.I. Simonov, Kristalografiya 32 (1987) 682.
[18] G. Suresh, R. Ratheesh, V.U. Nayar, M. Ichikawa, Spectrochim. Acta A 52 (1996) 465.
[19] D. Abramic, J. Dolinsk, R. Blinc, L.A. Shuvalov, Phys. Rev. B 42 (1990) 442.
[20] Y. Matsuo, K. Takahashi, K. Hisada, S. Ikehata, J. Phys. Soc. Jpn. 68 (1999) 2965.
[21] Y. Matsuo, K. Takahashi, S. Ikehata, J. Phys. Soc. Jpn. 70 (2001) 2934.
[22] I.P. Makarova, I.A. Verin, N.M. Shchagina, Sov. Phys. Crystallogr. 31 (1986) 105.
[23] R. Melzer, R. Sonntag, K.S. Knight, Acta Cryst. C 52 (1996) 1061.
[24] T. Gustafsson, M. Ichikawa, I. Olovsson, Solid State Commun. 115 (2000) 473.
[25] R. Melzer, T. Wessels, M. Reehuis, Solid State Ion. 92 (1996) 119.
[26] A. Abragam, The Principles of Nuclear Magnetism, Oxford University Press, Oxford, 1961.
[27] J. Dolinsek, U. Mikac, J.E. Javorsek, G. Lahajnar, R. Blinc, L.F. Kirpichnikova, Phys. Rev. B 58 (1998) 8445.
[28] S. Takeda, F. Kondoh, N. Nakamura, K. Yamaguchi, Physica B 226 (1996) 157.
[29] G. Bonera, F. Borsa, A. Rigamonti, Phys. Rev. B 21 (1970) 2784.
[30] S. Towta, D.G. Hughes, J. Phys.: Condens. Matter 2 (1990) 2021.
[31] Y. Matsumoto, J. Phys. Soc. Jpn. 67 (1998) 2215.